

Kent Academic Repository

Full text document (pdf)

Citation for published version

Arola, E. and Strange, Paul (1998) Application of relativistic scattering theory of x rays to diffraction anomalous fine structure in Cu. *Physical Review B: Condensed Matter and Materials Physics*, 58 (12). pp. 7663-7667. ISSN 0163-1829.

DOI

<https://doi.org/10.1103/PhysRevB.58.7663>

Link to record in KAR

<http://kar.kent.ac.uk/50038/>

Document Version

Publisher pdf

Copyright & reuse

Content in the Kent Academic Repository is made available for research purposes. Unless otherwise stated all content is protected by copyright and in the absence of an open licence (eg Creative Commons), permissions for further reuse of content should be sought from the publisher, author or other copyright holder.

Versions of research

The version in the Kent Academic Repository may differ from the final published version.

Users are advised to check <http://kar.kent.ac.uk> for the status of the paper. **Users should always cite the published version of record.**

Enquiries

For any further enquiries regarding the licence status of this document, please contact:

researchsupport@kent.ac.uk

If you believe this document infringes copyright then please contact the KAR admin team with the take-down information provided at <http://kar.kent.ac.uk/contact.html>

Application of relativistic scattering theory of x rays to diffraction anomalous fine structure in Cu

E. Arola* and P. Strange

Physics Department, Keele University, Keele, Staffordshire ST5 5BG, United Kingdom

(Received 8 January 1998)

We apply our recent first-principles formalism of magnetic scattering of circularly polarized x rays to a single Cu crystal. We demonstrate the ability of our formalism to interpret the crystalline environment related near-edge fine structure features in the resonant x-ray scattering spectra at the Cu K absorption edge. We find good agreement between the computed and measured diffraction anomalous fine structure features of the x-ray scattering spectra. [S0163-1829(98)03836-3]

I. INTRODUCTION

Since the observation of a large enhancement of x-ray magnetic scattering at the L_{III} absorption edge of the spiral antiferromagnet holmium by Gibbs *et al.*,¹ there has been an enormous increase in the use of synchrotron radiation sources in the study of structural and magnetic properties of materials.

X-ray resonant magnetic scattering (XRMS) has been applied to study the nature of magnetic coupling between Ni layers in a Ag/Ni multilayer,² to observe antiferromagnetically and long-range ordered Nd moments in an electron-carrier high- T_C superconductor precursor Nd_2CuO_4 .³ More recently, Chakarian *et al.*⁴ have applied the XRMS technique in a specular reflection geometry to a FeCo/Mn/FeCo multilayer and demonstrated its sensitivity to the chemical, magnetic, and layered structures. Déchelette-Barbara *et al.*⁵ have applied XRMS in specular reflection and diffraction geometries to understand the relationship between magnetic and structural phase transitions, and coherence properties in $Fe_xMn_{1-x}/Ir(001)$ superlattices.

One of the unique advantages of the XRMS technique over other x-ray techniques is that it is highly atom specific. In contrast, the more conventional x-ray-nonresonant magnetic scattering (XNRMS) is in general several orders of magnitude weaker than charge (or resonant) scattering and is not species selective. Nevertheless, using a polarization analysis of the measured beam intensity in suitable geometries, in connection with the XNRMS theory by Blume and Gibbs,⁶ Langridge *et al.*⁷ were able to estimate the orbital to spin (local) moment ratio in the type-IA²⁻⁹ antiferromagnetic UAs crystal.

It should be noted that in the above-mentioned studies the emphasis has been in observing charge/magnetic scattering intensity at the absorption edges of interest, but no attention was paid to exploiting the fine-structure features of the spectra present in the close vicinity of the absorption edge.

Recently, a completely new type of a x-ray-scattering probe, diffraction anomalous fine-structure (DAFS), has been suggested by Stragier *et al.*,⁸ and applied by Pickering *et al.*⁹ to several polycrystalline samples and by Renevier *et al.*¹⁰ to an Fe/Ir(100) superlattice in order to provide local atomic structural information. In DAFS studies the main focus is on the oscillatory, ‘‘photoelectron backscattering’’ features of the spectra, appearing close to the absorption edge of a given constituent atom. Stragier *et al.*⁸ have clearly dem-

onstrated that DAFS can accurately provide the same structural information as the more traditionally used x-ray-absorption fine-structure (XAFS) technique.

We have recently developed a first-principles formalism of magnetic scattering of x rays in the framework of the fully relativistic spin-polarized Korringa-Kohn-Rostoker (KKR) type multiple-scattering theory,¹¹ which treats spin-orbit interaction and spin-polarization effects on an equal footing. However, the most remarkable feature of our method, which we want to demonstrate, is that it includes the contribution of the crystalline environment to the scattering amplitude via the Green’s function expression of the multiple scattering theory in one-particle local-density approximation (LDA),¹¹ which allows an accurate implementation of the theory. Therefore, we should be able to see the characteristically oscillating DAFS features accurately in our calculated x-ray scattering spectra, without having to introduce a concept of an ‘‘oscillatory’’ function $\chi(\hbar\omega)$ and its approximate form (see Ref. 8) to describe the local structural contribution to the x-ray scattering amplitude.¹²

II. OUTLINE OF THE THEORY

We briefly describe the part of our relativistic x-ray scattering theory that is relevant for the DAFS studies at the K absorption edge of Cu, and then compare our computed real part of the ‘‘atomic form factor’’ with the one measured by Stanglmeier *et al.*¹⁴ As we showed in Ref. 11 the relativistic Bragg scattering amplitude (due to positive-energy excitations only¹³) for an ordered crystal within the KKR-type multiple-scattering theory can be written as (SI system of units used throughout)

$$f^{(\text{pos})}(\omega) = [f_0^{+(\text{pos})}(\omega) + f_0^{-(\text{pos})}(\omega)] N_{\text{atoms}} \delta_{\vec{Q}\vec{K}}, \quad (1a)$$

where $\vec{Q} \equiv \vec{q}' - \vec{q}$, \vec{K} is a reciprocal lattice vector of the crystal, $\delta_{\vec{Q}\vec{K}}$ is a Kronecker delta function, subscript 0 is a lattice-site index, and the resonant $[f_0^{+(\text{pos})}(\omega)]$ and nonresonant $[f_0^{-(\text{pos})}(\omega)]$ parts of the amplitude are given by

$$f_0^{+(-)\text{(pos)}}(\omega) = \sum_{\Lambda_0} f_{\Lambda_0; \vec{q}\lambda; \vec{q}'\lambda'}^{+(-)\text{(pos)}}(\omega), \quad (1b)$$

where $\lambda(\lambda')$ and $\vec{q}(\vec{q}')$ represent the polarization and the wave vector of the incident (outgoing) photon, respectively.

The Λ_0 -core-state contribution to the resonant amplitude is

$$f_{\Lambda_0; \vec{q}\lambda; \vec{q}'\lambda'}^{+(\text{pos})}(\omega) = - \sum_{\Lambda\Lambda'} \int_{\epsilon_F}^{\infty} \frac{d\epsilon}{\pi} \frac{m_{\Lambda_0}^{\Lambda+}(\vec{q}'\lambda'; \epsilon) \text{Im} \tau_{\Lambda\Lambda'}^{00}(\epsilon) m_{\Lambda_0}^{\Lambda'+*}(\vec{q}\lambda; \epsilon)}{\epsilon_{\Lambda_0} - \epsilon + \hbar\omega + i\Gamma/2}, \quad (2a)$$

and the Λ_0 -core-state contribution to the nonresonant amplitude is

$$f_{\Lambda_0; \vec{q}\lambda; \vec{q}'\lambda'}^{-(\text{pos})}(\omega) = - \sum_{\Lambda\Lambda'} \int_{\epsilon_F}^{\infty} \frac{d\epsilon}{\pi} \frac{m_{\Lambda_0}^{\Lambda-}(\vec{q}\lambda; \epsilon) \text{Im} \tau_{\Lambda\Lambda'}^{00}(\epsilon) m_{\Lambda_0}^{\Lambda'-*}(\vec{q}'\lambda'; \epsilon)}{\epsilon_{\Lambda_0} - \epsilon - \hbar\omega}. \quad (2b)$$

In Eqs. (2a) and (2b) Γ , the only adjustable parameter in the theory, represents the natural width of the intermediate states, $\text{Im} \tau_{\Lambda\Lambda'}^{00}(\epsilon)$ is the imaginary part of the $\Lambda\Lambda'$ [$\Lambda \equiv (\kappa m_j)$] element of the path operator matrix τ^{00} at energy ϵ , and ϵ_{Λ_0} is a core-state eigenvalue of the Dirac equation for a muffin-tin potential at site \vec{R}_0 .

The matrix element $m_{\Lambda_0}^{\Lambda+}(\vec{q}\lambda; \epsilon)$ of Eq. (2a), responsible for the resonant scattering, is defined by

$$m_{\Lambda_0}^{\Lambda+}(\vec{q}\lambda; \epsilon) \equiv \int_{\vec{r}_0 \in \Omega_0} u_{\Lambda_0}^{\dagger}(\vec{r}_0) X_{\vec{q}\lambda}^{\dagger}(\vec{r}_0) Z_{\Lambda}(\vec{r}_0, \epsilon) d^3 r_0, \quad (3a)$$

and the matrix element $m_{\Lambda_0}^{\Lambda-}(\vec{q}\lambda; \epsilon)$ of Eq. (2b), responsible for the nonresonant scattering, is defined by

$$m_{\Lambda_0}^{\Lambda-}(\vec{q}\lambda; \epsilon) \equiv \int_{\vec{r}_0 \in \Omega_0} u_{\Lambda_0}^{\dagger}(\vec{r}_0) X_{\vec{q}\lambda}(\vec{r}_0) Z_{\Lambda}(\vec{r}_0, \epsilon) d^3 r_0. \quad (3b)$$

In Eqs. (3a) and (3b) $u_{\Lambda_0}(\vec{r}_0)$ is a core-state solution of the magnetic Dirac equation at site \vec{R}_0 , $X_{\vec{q}\lambda}(\vec{r}) \equiv -e[\hbar c^2 / (2V\epsilon_0\omega_q)]^{1/2} \vec{\alpha} \cdot \hat{\epsilon}^{(\lambda)} e^{iq \cdot \vec{r}}$ [Eq. (9b) of Ref. 11] defines the relativistic photon-electron interaction vertex ($\hat{\epsilon}^{(\lambda)}$ is a unit, complex polarization vector of the photon with the polarization state λ), $Z_{\Lambda}(\vec{r}_0, \epsilon)$ is the regular scattering solution of the spin-polarized Kohn-Sham-Dirac equation, and $\vec{r}_0 \equiv \vec{r} - \vec{R}_0$ is the vector inside the unit cell Ω_0 at the origin. As shown in Ref. 11 numerically tractable expressions and selection rules can easily be derived to these matrix elements due the electric dipole ($E1$) or magnetic dipole and electric

quadrupole ($M1 + E2$) contributions to $X_{\vec{q}\lambda}(\vec{r})$. According to our initial computations, in the case of resonant scattering at the K edge of Cu, the ($M1 + E2$) contribution to the scattering amplitude is at least two orders of magnitude smaller than the $E1$ contribution. Therefore, we ignore it and use only the $E1$ approximation in our calculations.

The electronic structure part of the calculation has been carried out using a Cu muffin-tin potential derived from an all-electron charge self-consistent Korringa-Kohn-Rostoker code by Kaprzyk and Bansil¹⁵ for the Cu fcc lattice ($a = 6.76$ a.u.) and $l_{\text{max}} = 3$.

The relationship between the x-ray scattering amplitude $f(\omega)$ defined as the left-hand side of Eq. (9a) of Ref. 11 and the x-ray scattering form factor $f_{s-f}(\omega)$ will be briefly derived in the following. Including only those intermediate states $|I\rangle$ with excitations from the positive-energy single-particle core or conduction-band states ($\epsilon_{\Lambda} > 0$) we get for the relativistic scattering amplitude¹⁶

$$f^{(\text{pos})}(\omega) = \sum_{I, \epsilon_{\Lambda} > 0} \frac{\langle f | H'_{\text{int}} | I \rangle \langle I | H'_{\text{int}} | i \rangle}{E_i - E_I}, \quad (4)$$

where $|i\rangle$, $|f\rangle$, and $|I\rangle$ are the initial, final, and intermediate states of the electron-photon system, respectively, and E_i and E_I are the corresponding energies of the initial and intermediate states. By expressing the time-independent part of the relativistic photon-electron interaction operator H'_{int} in terms of the radiation field operator $\vec{A}(\vec{r})$ and the quantized Dirac field operators $\psi(\vec{r})$ and $\psi^{\dagger}(\vec{r})$ [cf. Eqs. (3) and (4) of Ref. 11] it is a straightforward matter to show that the positive-energy part of the elastic scattering amplitude can be written as

$$\begin{aligned} f^{(\text{pos})}(\omega) &= \frac{e^2 c^2 \hbar}{2V\epsilon_0\omega} \frac{1}{mc^2} \\ &\times \left[mc^2 \sum_{\Lambda\Lambda'} \left\{ \frac{\langle i_{\text{el}}^{\Lambda} | \vec{\alpha} \cdot \hat{\epsilon}^{(\lambda')} e^{-iq' \cdot \vec{r}} | I_{\text{el}}^{\Lambda'} \rangle \langle I_{\text{el}}^{\Lambda'} | \vec{\alpha} \cdot \hat{\epsilon}^{(\lambda)} e^{iq \cdot \vec{r}} | i_{\text{el}}^{\Lambda} \rangle}{\epsilon_{\Lambda} - \epsilon_{\Lambda'} + \hbar\omega} + \frac{\langle i_{\text{el}}^{\Lambda} | \vec{\alpha} \cdot \hat{\epsilon}^{(\lambda)} e^{iq \cdot \vec{r}} | I_{\text{el}}^{\Lambda'} \rangle \langle I_{\text{el}}^{\Lambda'} | \vec{\alpha} \cdot \hat{\epsilon}^{(\lambda')} e^{-iq' \cdot \vec{r}} | i_{\text{el}}^{\Lambda} \rangle}{\epsilon_{\Lambda} - \epsilon_{\Lambda'} - \hbar\omega} \right\} \right] \\ &\equiv f^{+(\text{pos})}(\omega) + f^{-(\text{pos})}(\omega), \end{aligned} \quad (5)$$

where the resonant [$f^{+(\text{pos})}(\omega)$] and nonresonant [$f^{-(\text{pos})}(\omega)$] amplitudes have been defined in terms of the one-electron initial core/band states $|i_{\text{el}}^{\Lambda}\rangle$ (occupied) and intermediate band states $|i_{\text{el}}^{\Lambda'}\rangle$ (empty), and the corresponding eigenenergies ϵ_{Λ} and $\epsilon_{\Lambda'}$ of the crystal Hamiltonian.¹⁷

The expression inside the square brackets of Eq. (5) can be identified as a relativistic x-ray scattering form factor $f_{s-f}(\omega)$ (cf. the relativistic atomic form factor expression of Cromer and Liberman¹⁸ for an isolated atom [Eq. (2) of Ref. 18]). Therefore, $f_{s-f}(\omega)$ for the solid can be written as

$$f_{s-f}(\omega) = K' [f_0^{+(\text{pos})}(\omega) + f_0^{-(\text{pos})}(\omega)], \quad (6)$$

where $K' \equiv 2\epsilon_0 m V \omega / (e^2 \hbar)$. The radiation field normalization volume V and angular-frequency ω dependence of factor K' will be canceled by the $\sim 1/(V\omega)^{1/2}$ dependence of the photon-electron interaction vertex $X_{q\lambda}(\vec{r})$ in the matrix elements of Eqs. (2a) and (2b).

To make contact with the experimental atomic form factor measurement for Cu,¹⁴ we have to make a few things clear. First, in the relativistic scattering amplitude expression [Eq. (1a)] there are two terms: a resonant and nonresonant one, both of which depend on photon energy, while in the nonrelativistic theory the scattering amplitude $f(\omega) = f^0 + f^+(\omega) + f^-(\omega)$ contains three terms: the frequency-independent charge (Thomson) term f^0 , and frequency-dependent resonant [$f^+(\omega)$] and nonresonant [$f^-(\omega)$] amplitudes. Second, Stanglmeier *et al.*¹⁴ have done small-angle x-ray reflectivity measurements from several metal- and metal-oxide surfaces. Combining the nonrelativistic atomic form factor (cf. scattering amplitude) expression, the complex index of refraction dependence on the forward-scattering amplitude, and the classical electromagnetic reflectivity from a flat surface of a single- or multilayer system, they were able to extract the real part of the frequency-dependent dispersive correction to the atomic form factor [denoted as $f'(\omega)$ in their paper] in Cu. Therefore, it is clear that in order to make comparison between the experimentally determined¹⁴ dispersive correction to the atomic form factor and our relativistically computed form factor, we have to subtract a constant value from the computed result. Furthermore, this constant is not directly related to the measured Thomson-scattering part of the amplitude (f^0), because we have computed only the K absorption edge contribution to the scattering amplitude. However, the constant shift of our computed scattering amplitude is justified as all electrons of the atoms in the unit cell have a frequency-independent contribution to the Thomson amplitude. We want to emphasize that the near-edge (DAFS) features in the x-ray scattering spectra are due to excitations (intermediate states) where only one particular atomic core level is involved, and higher core- and filled valence Bloch states give a smooth and nonoscillatory behavior to the spectra.

III. RESULTS AND DISCUSSION

In Fig. 1 we show the real part of the dispersive correction [$f'(\omega)$] to the atomic form factor at Cu K absorption edge, based on the small-angle reflectivity measurement¹⁴ together with our computed “atomic form factor,” which has been shifted by a constant value of about -6 .

As can be seen from Fig. 1 the smoothly decreasing part of the computed $f'(\omega)$ towards the cusp at the K absorption edge (about 8980 eV according to the present experiment) is in qualitative agreement with the experimentally determined f' values. But the most remarkable observation is that our first-principles calculation of x-ray scattering from copper crystal is able to reproduce DAFS related fine-structure features observed in the measured $f'(\omega)$ in the photon energy interval [8982 eV, 8992 eV]. Even the dip feature D of Fig. 1 at photon energy of about 8989 eV is well reproduced by the calculation. We also notice that the sharply rising tail above $\hbar\omega = 8992$ eV is also apparent in our computed f' spectra. Nevertheless, as can be seen from Fig. 1, the computed real part of the form factor is not in perfect quantitative agreement with the experimentally determined form factor. Obvious sources for this disagreement are listed in the following. (i) According to Stanglmeier *et al.* the main factor limiting the accuracy of their measurement is the error in determining the angle of incidence (grazing angle with respect to the surface). They have estimated error limits of ± 0.3 (electrons) around $f'(\omega)$ for a photon energy range of 7.6 to 13 keV. (ii) Our forward scattering form factor calculation is strictly valid for bulk Cu only. On the other hand, the measurements in Ref. 14 have been done in the range of total reflection. Therefore, the DAFS oscillations measured in $f'(\omega)$ spectra are likely to have contributions from surface electronic structure. Also their approximately 1000-Å-thick Cu sample is covered by a thin 35-Å oxide layer. This may well change the nature of the electron states above the Fermi energy (cf. intermediate states of the scattering process) with a direct effect onto the x-ray scattering spectra close to the absorption edge. (iii) Some of the tiny DAFS-like features present in our calculated $f'(\omega)$ spectra have probably been washed out in the experimental spectra due to the monochromator energy pass band width of 1.5 eV at 10 keV.¹⁴ (iv) Although the oversimplified way of dealing with many-body

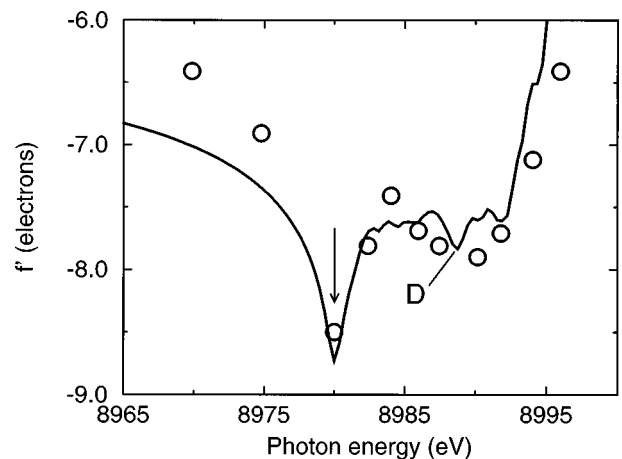


FIG. 1. Real part [$f'(\omega)$] of the calculated relativistic anomalous scattering form factor in electric dipole ($E1$) approximation at the Cu K edge, shifted by a constant amount in the vertical direction (solid line) (see discussion in the text). The incoming and scattered photons propagate in the same direction. The measured dispersive correction (open circles) to the atomic form factor from the x-ray reflection measurement has been reproduced from Fig. 18 of Stanglmeier *et al.* (Ref. 14). The arrow locates the position of the experimental K edge.

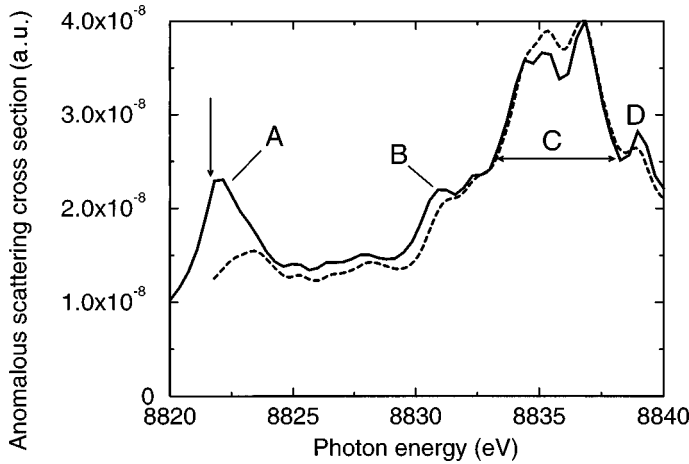


FIG. 2. Calculated anomalous scattering cross section at the copper K absorption edge in $E1$ approximation (solid line). The relativistic p -projected density of states has been Lorentz-convolved ($\Gamma=1$ eV), squared, and normalized according to the maximum value of peak C (dashed line). The arrow locates the position of the computed K absorption edge.

effects via the core-hole lifetime broadening parameter Γ [cf. Eq. (2a)] is in common use, going beyond this would certainly improve further the quality of the computed scattering spectra.

We briefly turn to discuss the computed anomalous scattering cross section $d\sigma/d\Omega = |f(\omega)|^2 V^2 \omega^2 / (2\pi\hbar c^2)^2$ in the electric dipole ($E1$) approximation at the copper K absorption edge in Fig. 2. To demonstrate crystal environment effects on the scattering cross section, we display in Fig. 2 also the Lorentz-convolved ($\Gamma=1$ eV) and squared p -projected density of states (DOS). The near-edge behavior of the scattering cross section in favorable conditions can be qualitatively described by a squared value of the partial DOS above the Fermi level.¹¹ And indeed, we found a lot of similarities between these two curves at iron K edge. But interestingly, we notice from Fig. 2 that in the case of elastic, resonant scattering of x rays at the Cu K edge, there is an even more striking similarity between the cross section and the Lorentz-convolved and squared Cu p density of states.

The connection between the cross section and a partial density of states can be delineated in terms of the following facts.¹¹ (i) The matrix elements of Eq. (2a) are in general smooth functions of band energy ϵ . According to the selection rules of the relativistic x-ray scattering theory in $E1$ approximation,¹¹ the only matrix elements that contribute to scattering at the K absorption edge are those with the transitions¹⁹ $(s_{1/2}, -1/2) \rightarrow (p_{1/2}, +1/2)$, $(s_{1/2}, -1/2) \rightarrow (p_{3/2}, +1/2)$, and $(s_{1/2}, +1/2) \rightarrow (p_{3/2}, +3/2)$ in the (κ, m_j) representation. Therefore, as a good approximation, only the p -state-related $\text{Im } \tau_{\Lambda\Lambda}^{00}(\epsilon)$ elements are responsible for building the scattering amplitude of Eq. (2a). (ii) The numerator part of Eq. (2a) will be then approximately proportional to the p -projected density of states.¹¹ (iii) Provided the lifetime parameter Γ of Eq. (2a) is small enough compared to the width of the p density of states features above Fermi energy, and the conditions (i)–(ii) are satisfied, then the computed x-ray scattering cross section $d\sigma/d\Omega$ should closely follow the shape of the Lorentz-convolved and squared p -projected density of states.

Many spectroscopic features of the cross section can be qualitatively explained by looking numerically at the numerator part of Eq. (2a) above the Fermi level.¹¹ In case of the resonant scattering at the K edge of Cu, there are three major channels [cf. the numerator part of Eq. (2a)], which contribute to build up the features A – D of Fig. 2. A detailed study shows that these three major channels, which contribute to those features with nearly equal relative weights, contain transitions: $(s_{1/2}, +1/2) \rightarrow (p_{3/2}, +3/2)$ (strongest), $(s_{1/2}, -1/2) \rightarrow (p_{1/2}, +1/2)$ (next strongest), and $(s_{1/2}, -1/2) \rightarrow (p_{3/2}, +1/2)$ (weakest contribution). All matrix elements with these transitions are linked with diagonal path operator matrix elements $\tau_{\Lambda\Lambda}^{00}$ in Eq. (2a). We notice furthermore that the “shoulder” feature B of Fig. 2 can directly be linked to the “dip” feature D in the $f'(\omega)$ spectra of Fig. 1 when combined with the imaginary part $f''(\omega)$ (not shown) of the complex form factor at the same energy.

IV. CONCLUSIONS

In conclusion, we have demonstrated that it is possible to interpret diffraction anomalous fine structure (DAFS) features by using a x-ray scattering calculation based on a *first-principles* LDA electron structure theory. We base our expertise on our recently developed relativistic x-ray magnetic scattering formalism.¹¹ As it appears, our computed dispersion correction spectra [$f'(\omega)$] for Cu crystal around the K edge agrees well with the measured one, and especially the DAFS related features of the measured spectra can be reproduced, at least, qualitatively.

In spite of the inherently fundamental restrictions in our method (like LDA approach describing the intermediate Bloch states in the x-ray scattering process), it is obvious that a higher resolution synchrotron reflectivity measurement used in connection with a more accurate way of determining $f'(\omega)$ (like x-ray interferometry technique), would improve the agreement between experimentally and computationally determined $f'(\omega)$ further.

We have implemented our general x-ray scattering amplitude expression [Eq. (11) of Ref. 11] in the simplest possible environment, which is a perfect, infinite crystal. As we have shown,²⁰ x-ray magnetic scattering, including DAFS features for a completely random magnetic alloy, can easily be implemented using the coherent-potential-approximation (CPA) in context of Eq. (11) of Ref. 11.

We hope that the results presented in this paper for the Cu K edge will stimulate further development of DAFS as an experimental tool for probing the electronic structure of more complex materials. A very interesting development of our theory would be to implement it for short-range order and complicated magnetic structure studies. A feasible and accurate way of doing this would be to use recently developed electronic structure methods with order- N scaling properties like the locally self-consistent multiple scattering (LSMS) method by Wang *et al.*,²¹ or the locally self-consistent Green’s function (LSGF) approach by Abrikosov *et al.*²² These first-principles methods can describe accurately electronic structures of large crystalline random or ordered systems, or systems with short-range order.

- ^{*}Present address: Department of Physics, University of Bath, Bath BA2 7AY, United Kingdom.
- ¹D. Gibbs, D. R. Harshman, E. D. Isaacs, D. B. McWhan, D. Mills, and C. Vettier, *Phys. Rev. Lett.* **61**, 1241 (1988).
- ²J. M. Tonnerre, L. Sève, D. Raoux, G. Soullié, B. Rodmacq, and P. Wolfers, *Phys. Rev. Lett.* **75**, 740 (1995).
- ³J. P. Hill, A. Vigliante, D. Gibbs, J. L. Peng, and R. L. Greene, *Phys. Rev. B* **52**, 6575 (1995).
- ⁴V. Chakarian, Y. U. Idzerda, C.-C. Kao, and C. T. Chen, *J. Magn. Magn. Mater.* **165**, 52 (1997).
- ⁵A. Déchelette-Barbara, J. M. Tonnerre, M. C. Saint-Lager, F. Bartolomé, J. F. Bézar, D. Raoux, H. M. Fischer, M. Piecuch, V. Chakarian, C. C. Kao, M. Gailhanou, S. Lefèvre, and M. Besière, *J. Magn. Magn. Mater.* **165**, 87 (1997).
- ⁶M. Blume and D. Gibbs, *Phys. Rev. B* **37**, 1779 (1988).
- ⁷S. Langridge, G. H. Lander, N. Bernhoeft, A. Stunault, C. Vettier, G. Grübel, C. Sutter, F. de Bergevin, W. J. Nuttall, W. G. Stirling, K. Mattenberger, and O. Vogt, *Phys. Rev. B* **55**, 6392 (1997).
- ⁸H. Stragier, J. O. Cross, J. J. Rehr, L. B. Sorensen, C. E. Bouldin, and J. C. Woicik, *Phys. Rev. Lett.* **69**, 3064 (1992).
- ⁹I. J. Pickering, M. Sansone, J. Marsch, and G. N. George, *J. Am. Chem. Soc.* **115**, 6302 (1993).
- ¹⁰H. Renevier, J. L. Hodeau, P. Wolfers, S. Andrieu, J. Weigelt, and R. Frahm, *Phys. Rev. Lett.* **78**, 2775 (1997).
- ¹¹E. Arola, P. Strange, B. L. Gyorffy, *Phys. Rev. B* **55**, 472 (1997).
- ¹²We want to emphasize that we solve the x-ray-scattering spectra from first principles for a given structure (in our case a perfect, infinite Cu crystal), while Stragier *et al.*⁸ solve the inverse problem: using the measured spectra in combination with a model oscillating DAFS contribution $\chi(\hbar\omega)$ to the spectra and the Fourier transform of the DAFS signal, they are able to extract a local structural real space information of Cu crystal.
- ¹³The negative-energy states can be ignored using the same arguments as given in the end of Sec. II C of Ref. 11 in the case of the x-ray resonant scattering from iron.
- ¹⁴F. Stanglmeier, B. Lengeler, W. Weber, H. Göbel, and M. Schuster, *Acta Crystallogr., Sect. A: Found. Crystallogr.* **48**, 626 (1992).
- ¹⁵S. Kaprzyk and A. Bansil, *Phys. Rev. B* **42**, 7358 (1990); A. Bansil and S. Kaprzyk, *ibid.* **43**, 10 335 (1991).
- ¹⁶Our definition of the scattering amplitude $[f^{(\text{our})}(\omega)]$ differs slightly from the standard one $[f^{(\text{std})}(\omega)]$ defined by the differential scattering cross section $d\sigma/d\Omega \equiv |f^{(\text{std})}(\omega)|^2$. They are connected by the relation $f^{(\text{std})}(\omega) = f^{(\text{our})}(\omega) V\omega/(2\pi\hbar c^2)$ [see Sec. III A and Ref. 25 in Ref. 11].
- ¹⁷For small enough photon energies or a small-angle scattering geometry the electron momentum transfer is negligible as compared to the dimensions of the Brillouin zone. Therefore, the final electron state can be assumed to be identical to the initial electron state. In fact, this is exactly true in our x-ray scattering geometry as we assume the incoming and scattered photons to propagate in the same direction.
- ¹⁸D. T. Cromer and D. Liberman, *J. Chem. Phys.* **53**, 1891 (1970).
- ¹⁹We assume that both the incoming and outgoing beams have positive helicity ($\lambda = +$). Changing the helicities of these beams to negative ($\lambda = -$) has virtually no affect on the cross section, because the dichroic effects are very minor due to small spin-orbit and exchange interactions in copper crystal.
- ²⁰E. Arola, P. Strange, N. I. Kulikov, M. J. Woods, and B. L. Gyorffy, *J. Magn. Magn. Mater.* **177-181**, 1415 (1998).
- ²¹Y. Wang, G. M. Stocks, W. A. Shelton, D. M. C. Nicholson, Z. Szotek, and W. M. Temmerman, *Phys. Rev. Lett.* **75**, 2867 (1995).
- ²²I. A. Abrikosov, A. M. N. Niklasson, S. I. Simak, B. Johansson, A. V. Ruban, and H. L. Skriver, *Phys. Rev. Lett.* **76**, 4203 (1996).